Phosphorescence and Optically Detected Magnetic Resonance Characterization of the Environments of Tryptophan Analogues in Staphylococcal Nuclease, Its V66W Mutant, and Δ137−149 Fragment†

Andrzej Ozarowski,‡ Jie Q. Wu,‡ Sara K. Davis,‡ Cing-Yuen Wong,§ Maurice R. Eftink,*,§ and August H. Maki*,‡

Departments of Chemistry, University of California, Davis, Davis, California 95616, and University of Mississippi, University, Mississippi 38677

Received July 30, 1997; Revised Manuscript Received April 21, 1998

ABSTRACT: Phosphorescence and optically detected magnetic resonance (ODMR) measurements are reported on the triplet states of the tryptophan analogues, 7-azatryptophan (7AW), 5-hydroxytryptophan (5HW), and 4-, 5-, and 6-fluorotryptophan (4FW, 5FW, 6FW), when incorporated at position 140 of wild-type Staphylococcal nuclease (7AW-nuclease, etc.), positions 66 and 140 of its V66W mutant (7AW-V66W, etc.), and the deletion fragment of the latter, Δ137−149 (7AW-V66W′, etc.). These measurements point to the retention of protein structure at position 140 in each of the wild-type nuclease analogues. Substitution of the analogue at both tryptophan sites of V66W leads to structured sites with differentiated triplet-state properties for all analogues except 7AW-V66W, whose structure is destabilized. 5HW-V66W′ is the only fragment that apparently lacks structure at position 66. All other V66W′ analogues exhibit a structured environment at position 66 (4FW-V66W′ was not studied), but in each case this site can be differentiated readily from the corresponding site in intact V66W. 7AW-V66W′ is resolved by ODMR into two discrete structures with slightly differing zero field splittings (ZFS). Interaction of the protein with 5HW at position 66 of 5HW-V66W induces a 2-fold increase in the ZFS *E* parameter, which is reduced to its normal value upon formation of the fragment, 5HW-V66W′. Analogous effects occur for 5FW, but on a smaller scale.

There is a growing practice of using biosynthetically incorporated tryptophan analogues as "intrinsic" probes of protein local structure (*1*−*10*). These tryptophan analogues include 5-hydroxytryptophan (5HW),[1] 7-azatryptophan (7AW), 4-fluorotryptophan (4FW), 5-fluorotryptophan (5FW), and 6-fluorotryptophan (6FW). Several of these analogues have features that make them useful as optical (fluorescence/absorbance) probes (*4*, *9*); the fluorotryptophans are useful as ^{19}F NMR probes (*5*−*7*). For example, 5HW, 7AW, and 5FW have absorbance spectra that extend to longer wavelengths than does tryptophan itself, enabling preferential excitation of the analogue in fluorescence experiments. Furthermore, the fluorescence of 5HW is insensitive to its environment, in contrast with 7AW, whose fluorescence is very sensitive to its environment. The absorbance of 4FW is blue-shifted with respect to that of tryptophan, and it has a low fluorescence quantum yield, making this analogue useful for cases in which it is desirable to greatly diminish the fluorescence of a particular tryptophan site (see, for instance, ref *9*, and citations therein).

While the fluorescence properties of the various tryptophan analogues are being studied in several laboratories, other spectroscopic methods that have the potential to provide much information about the local environment of the analogue are phosphorescence and optically detected magnetic resonance (ODMR), which involve the excited triplet state. These methods have yet to be applied to tryptophan analogue-containing proteins. Recently, one of our laboratories has initiated a study of the phosphorescence and ODMR of some tryptophan analogues as free amino acids in solution (*11*, *12*). The present study is designed to extend these triplet state methods to characterize the local environment of tryptophan analogues in proteins.

The proteins to be investigated are Staphylococcal nuclease, its V66W mutant, and the Δ137−149 fragment of the latter (referred to as V66W′). This set of proteins enables characterization of the spectroscopic properties of tryptophan (or analogue) at two distinct positions. The single Trp-140 is moderately solvent exposed in wild-type nuclease, whereas Trp-66 in V66W and V66W′ is an internal residue (*13*). The effect of the tryptophan analogues at either position 66 or position 140 on the stability of these proteins has been studied previously (*8*, *10*). To briefly summarize some of these

† This research was partially supported by Grant ES-02662 (AHM) from the National Institutes of Health and Grant MCB94-07167 (MRE) from the National Science Foundation.

* To whom correspondence should be addressed.

‡ University of California, Davis.

§ University of Misssissippi.

[1] Abbreviations: 7AW, 7-azatryptophan; *D* and *E*, zero field splitting parameters; EDTA, ethylenediamine tetraacetate; EEDOR, electron−electron double resonance; EG, ethylene glycol; 4FW, 5FW, and 6FW, 4-, 5-, and 6-fluorotryptophan; 5HW, 5-hydroxytryptophan; MIDP, microwave-induced delayed phosphorescence; nuclease, wild-type Staphylococcal nuclease; ODMR, optically detected (triplet state) magnetic resonance; slr, spin−lattice relaxation; V66W, mutated Staphylococcal nuclease; V66W′, Δ137−149 fragment of V66W; X-nuclease, wild-type Staphylococcal nuclease with amino acid X in position 140; X-V66W, Staphylococcal nuclease V66W mutant with amino acid X at positions 66 and 140; X-V66W′, 1−136 peptide fragment of X-V66W; ZFS, zero field splittings.

S0006-2960(97)01864-3 CCC: $15.00
Published on Web 06/06/1998

results, among the analogues being investigated, 7AW has a destabilizing effect on all three proteins, while 5HW appears to be destabilizing at position 66 of V66W′. The other analogues are either nonperturbing or slightly stabilizing at both positions of this set of proteins. Thus, the triplet state studies that are the subject of this paper are primarily for tryptophan analogues in nativelike structures of the alloproteins, although in a few cases the alloproteins are found to be unstructured by the stability and solution spectroscopic studies. Of interest in this report is how the triplet state methods sense structural/environmental differences between alloproteins containing analogues at positions 66 and 140.

What is known about the ODMR parameters of these tryptophan analogues and their sensitivity to environmental factors? In previous studies (*11*, *12*) we have learned that the zero field splittings (ZFS) and decay kinetics of the free amino acids, 5HW and 7AW, are changed significantly relative to tryptophan. 5-Hydroxyl substitution in tryptophan has the major effect of cutting the magnitude of the ZFS E parameter in half. Thus, the 2E transition has the lowest frequency in 5HW ($|D| > 3|E|$), while it is the central one in tryptophan ($|D| < 3|E|$). Relatively minor changes in ZFS are produced by 7-aza modification of tryptophan, on the other hand; $|E|$ increases while $|D|$ decreases somewhat. The ODMR linewidths of 5HW increase significantly relative to tryptophan, indicating larger solvent effects on the ZFS, while the reverse is true for 7AW. The peak frequency of the 2E transition of 5HW appears to be particularly sensitive to changes in local interactions, even varying significantly with respect to the emission wavelength that is monitored (A. Ozarowski, unpublished observations), which is a signature of strong solvent interactions (*14*). The major effect of 5-hydroxyl substitution on the kinetic parameters of tryptophan is to bring about a doubling of k_y so that it becomes more nearly comparable to k_x, while 7-aza substitution increases both k_x and k_y by comparable amounts, due to the introduction of a spin−orbit coupling mechanism involving the aza N-atom. In all three amino acids, tryptophan, 5HW, and 7AW, $k_z = 0$ within experimental error (± 0.01 s^{-1}), the T_z sublevel decaying largely by spin−lattice relaxation (slr) processes. No previous ODMR studies on the analogues, 4FW, 5FW, or 6FW, have been reported. The detailed triplet-state properties of these amino acids, both free and incorporated as tryptophan analogues in wild-type Staphylococcal nuclease, V66W, and V66W′, are reported here for the first time.

MATERIALS AND METHODS

Materials. The preparation of Staphylococcal nuclease, V66W, and V66W′, containing the various tryptophan analogues, has been described (*8*, *9*). These proteins are referred to as follows: 5HW-nuclease, 7AW-nuclease, and 4FW-, 5FW-, and 6FW-nuclease for wild-type nuclease containing the respective analogue; 5HW-V66W, 7AW-V66W, 4FW-, 5FW-, and 6FW-V66W for the V66W containing the analogue at positions 66 and 140; and 5HW-V66W′, 7AW-V66W′, and 4FW-, 5FW-, and 6FW-V66W′ for the V66W′ fragment containing the respective analogue at position 66. An estimate of the extent of incorporation of the analogues into these proteins has been given (*9*).

For phosphorescence and ODMR measurements, the concentrations of 5HW-nuclease, 4FW-, 5FW-, and 6FW-nucleases, 5HW-V66W, and 4FW-, 5FW-, and 6FW-V66W were about 0.6 mM, while 5HW-V66W′, 5FW-V66W′, and 6FW-V66W′ concentrations were about 0.7 mM. The proteins were dissolved in 40% (v/v) ethylene glycol (EG)/aqueous 10 mM pH 7 phosphate buffer containing 0.1 M NaCl and 10^{-4} M EDTA. These concentrations were estimated by weighing lyophilized samples using molar weights of 17 000 for 5HW-nuclease, the FW-nucleases, 5HW-V66W, and FW−V66W, while 15 500 was used for 5HW-V66W′ and FW-V66W′. The concentrations of 7AW-nuclease, 7AW-V66W′, and 7AW-V66W were 0.2 mM, 0.35 mM, and 0.2 mM, respectively, in a solution of the same buffer containing 30% (v/v) EG. These concentrations were determined by absorption spectroscopy using $\epsilon^{280} = 15.9 \times 10^3$ for 7AW-nuclease and 7AW-V66W′ and $\epsilon^{280} = 21.9 \times 10^3$ for 7AW-V66W. The amino acids 7AW (D,L), 5HW (L), and 6FW (D,L) were purchased from Sigma. 4FW and 5FW (D,L) were obtained from ICN. Samples were used as received and dissolved in EG/buffer, as detailed above, to a concentration of about 1 mM.

Methods. For phosphorescence and ODMR measurements, the samples were contained in a 1 mm i.d. Suprasil quartz tube placed in a helical copper slow-wave structure that terminated a 50 ohm stainless steel transmission line. The sample was placed into a stainless steel dewar with an optical tail for phosphorescence measurements at 77 K or for ODMR measurements at pumped liquid He temperature, about 1.2 K. Details of the experimental equipment and methods have been described recently (*11*, *12*, *15*). The samples were optically pumped using the output of a 100 W high-pressure Hg arc lamp passed through a 0.1 m monochromator set at a band-pass of 16 nm either centered at 295 nm for excitation of tryptophan as well as 7AW and 5HW or set at 313 nm for selective red-edge excitation of 7AW-containing proteins and at 320 nm for selective red-edge excitation of 5HW-containing proteins. For red-edge excitation of either 7AW- or 5HW-containing proteins, a WG 320-2 glass filter was inserted in the excitation path to eliminate all detectable emission from tryptophan. Milder red-edge excitation at 302 nm with 16 nm band-pass and a WG305-1 cutoff filter was used for all 5FW- and 6FW-containing samples while the 4FW-containing samples required 285 nm excitation. Emission was focused on a 1 m monochromator set for 3 nm band-pass for both phosphorescence and ODMR. To eliminate intense background fluorescence of tryptophan and of the 7AW and the fluoro derivatives, steady-state ODMR and phosphorescence measurements were made using a rotating sector. In the case of 5HW and its derivatives, the fluorescence background was sufficiently feeble that steady-state ODMR could be carried out without the sector.

Slow-passage ODMR signals obtained during continuous optical pumping (steady-state ODMR) were analyzed using a theoretical expression that compensates for distortions of the band shape caused by rapid-passage effects (*15*). The experimental data obtained from the $T_i \leftrightarrow T_j$ transition ($i, j = x, y, z$) between triplet sublevels, collected in a multichannel scaler (EG&G ORTEC, Inc., MCS-plus), are fitted to the expression

$$I(p\Delta\nu) = C' \sum_{n \le p} g_n\{\exp[-\kappa_i(p-n)] - R_{ji}\exp[-\kappa_j(p-n)]\} \quad (1)$$

using a Marquardt−Levenberg algorithm that minimizes χ^2. In eq 1, $I(p\Delta\nu)$ is the intensity of the ODMR signal in the pth channel while $\Delta\nu$ is the frequency width of a channel; n labels a channel $\le p$, $\kappa_{i,j} = k_{i,j}T/N$, $R_{ji} = k_j^{(r)}/k_i^{(r)}$, and $C' = Ck_i^{(r)}$. In the previous expressions, $k_{i,j}$ are the decay constants of $T_{i,j}$, $k_{i,j}^{(r)}$ are their radiative rate constants, N is the total number of channels in the data set, T is the time required to traverse the data set, C is a proportionality constant that depends on the degree of spin alignment as well as the experimental arrangement, and g_n is the inhomogeneously broadened band shape, assumed to be Gaussian

$$g_n = \exp(-\Gamma^2 n^2) = \exp[-(\nu - \nu_0)^2 \ln 2/\nu_{1/2}{}^2] \quad (2)$$

In eq 2, $\Gamma^2 = (\Delta\nu)^2 \ln 2/\nu_{1/2}{}^2$, and ν_0 and $\nu_{1/2}$ are the peak frequency and half-width at half-height of the distribution. Signal averaging was carried out typically over about 50 cycles. Equation 1 assumes that slr and the effects of optical pumping on the kinetic behavior of the triplet state can be ignored. This normally is not a reliable assumption, so the kinetic and radiative parameters obtained from the analysis are only approximations of the actual values; we do not report these here. The values of ν_0 and $\nu_{1/2}$ obtained from this treatment have been shown (*15*) to be very accurate, however.

Slow-passage ODMR measurements made during the decay of the triplet state after shuttering the exciting light (delay ODMR) are also included in this work. This experiment has the advantages over steady-state ODMR that interfering fluorescence is not present, eliminating the need for a rotating sector, and the spin alignment is often larger. This method is used in this paper to discriminate between signals whose intensities decay at different rates. The data are analyzed in the same manner as described above using an expression analogous to eq 1, which now includes an additional term describing the time dependence of the spin alignment as the triplet state sublevel populations decay (*11*). The same parameters, listed above, are obtained from this analysis; the kinetic and radiative parameters still are influenced by slr. Analysis of both steady-state ODMR and delay ODMR signals has been expanded in this paper to include two overlapping transitions provided that they originate from distinct (noninteracting) triplet states. Each of the parameters may be treated as variable, or fixed in the analysis, as desired.

All three of the expected ODMR transitions of 5HW and 7AW were measured in the samples reported in this work when possible. Their frequencies in terms of the D and E ZFS parameters are $\nu_0(D-E)$, $\nu_0(2E)$, and $\nu_0(D+E)$. In this work, we have calculated D and E from the experimental peak frequencies (ν_0), once they have been assigned, using

$$D = (^1/_2)[\nu_0(D-E) + \nu_0(D+E)] \quad (3)$$

and

$$E = (^1/_4)[\nu_0(D+E) + \nu_0(2E) - \nu_0(D-E)] \quad (4)$$

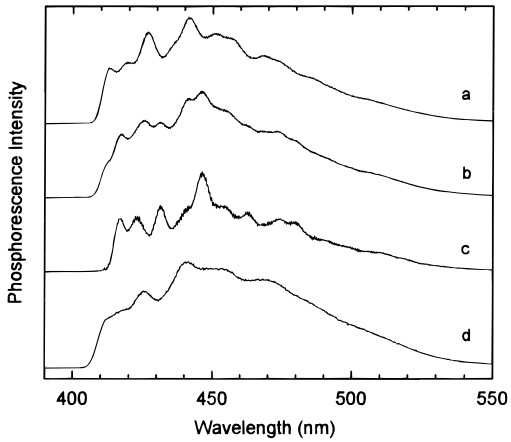

FIGURE 1: Phosphorescence spectra of (a) 5HW-nuclease, (b) 5HW-V66W, (c) 5HW-V66W minus 5HW-nuclease (see text), and (d) free 5HW amino acid at 77 K. Red-edge excitation was employed, see text.

Steady-state electron−electron double resonance (EEDOR) measurements (*16*) were carried out on some of the FW samples in order to enhance the $D + E$ ODMR transition. The $D + E$ frequency region was swept while continuously saturating the $D - E$ band.

We have pointed out previously (*11*) that the peak frequencies obtained from analysis of inhomogeneously broadened slow-passage ODMR bands are not always additive to within experimental error, that is, that the sum of the two lower peak frequencies does not add to that of the third, within the experimental error. Thus far, the deviation has been found to lie within the inhomogeneous bandwidth, however. We think that the problem is connected with the detailed nature of the inhomogeneous broadening process. It is possible that our assumption that the band shape is Gaussian is an oversimplification and that the actual band may not be symmetrical.

RESULTS

Phosphorescence of 5-Hydroxytryptophan in Staphylococcal Nuclease. The phosphorescence spectra of 5HW in 5HW-nuclease and in 5HW-V66W are shown in Figure 1, parts a and b, respectively. Red-edge excitation was used to obtain these spectra. When the excitation is shifted to the blue, a new 0,0-band origin with a peak at about 407 nm appears which is attributed to the presence of W-nuclease and W-V66W, respectively, in these samples (spectra not shown). When the emission is monitored at 407 nm, ODMR signals are observed (see below) that are identical to those reported previously (*13*) for these tryptophan-containing enzymes. The phosphorescence of 5HW-nuclease is similar to that of free 5HW (Figure 1d), except that it is more highly resolved. A prominent 0,0-band is observed at 413 nm. The spectrum of 5HW-V66W clearly has additional structure. A new band is found at 417 nm, which has no counterpart in the 5HW-nuclease emission, while a shoulder at about 413 nm is assigned as the 0,0-band of 5HW at position 140. The spectrum shown in Figure 1c is obtained by subtracting a scaled 5HW-nuclease spectrum from that of 5HW-V66W. Spectrum 1a is weighted so that it contributes half of the integrated intensity of the 5HW-V66W emission. This procedure yields an accurate representation of the phospho-

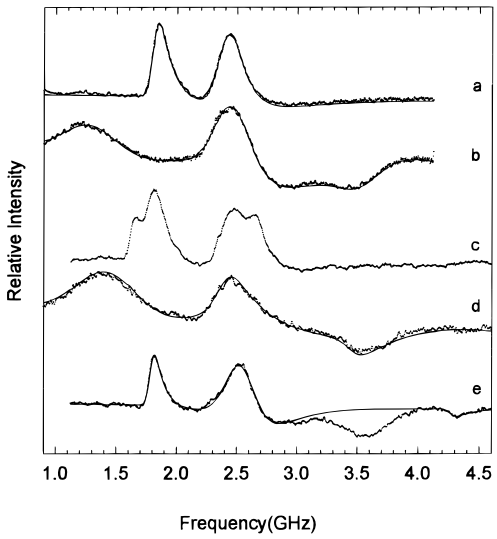

FIGURE 2: Steady-state ODMR spectra at 1.2 K of (a) and (b) 5HW-nuclease and (c, d, and e) 5HW-V66W. Excitation is at 295 nm, 16 nm band-pass, for a and c; red-edge excitation, see text, is used for b, d, and e. Emission is monitored at (a) 407, (b) 412, (c) 407, (d) 411, and (e) 417 nm using 3 nm bandwidth. The smooth curves in a, b, d, and e are a Marquardt−Levenberg fitting of the responses to eq 1 (*15*). The best-fit parameters, ν_0 and $\nu_{1/2}$, are listed in Table 1.

rescence of 5HW 66 to the extent that (a) there is no change in the 5HW-nuclease spectrum caused by mutation at position 66 and (b) the residues at positions 66 and 140 have the same quantum yield. The vibronic structure of the difference spectrum, Figure 1c, resembles that of 5HW-nuclease, except that it is more highly resolved and is shifted to the red by about 4 nm. We think that this spectrum is a good representation of the contribution of 5HW at position 66 to the phosphorescence of 5HW-V66W. Evidence from ODMR spectroscopy will be presented below that demonstrates that the 413 and 417 nm peaks of 5HW-V66W originate from 5HW in dissimilar environments.

The phosphorescence spectrum of 5HW-V66W′ (not shown) resembles that of the free 5HW amino acid, although it is even more poorly resolved. The highly resolved vibronic structure of Figure 1c that would be expected from an intact structured fragment is not observed, suggesting that structural integrity of 5HW-V66W is lost in forming the 1−136 fragment.

Optically Detected Magnetic Resonance of 5-Hydroxytryptophan and Tryptophan in Staphylococcal Nuclease. The steady-state ODMR spectra of the 5HW-nuclease and 5HW-V66W samples are shown in Figure 2. Excitation of either sample at 295 nm produces a blue-shifted 0,0-band at about 407 nm, as mentioned in the previous section, which we attribute to tryptophan in residual W-nuclease and W-V66W, respectively. Monitoring the emission at 406 nm yields the steady-state ODMR spectra shown in Figure 2a for 5HW-nuclease and Figure 2c for 5HW-V66W. These spectra are identical to those observed previously (*13*) from authentic samples of W-nuclease and W-V66W, respectively. The two tryptophan sites of W-V66W appear as resolved doublets (Figure 2c).

With red-edge excitation, the tryptophan emission is no longer seen; the phosphorescence spectra appear as shown in Figure 1, parts a and b. When 5HW-nuclease is monitored at the 413 nm 0,0-band peak, the steady-state ODMR spectrum shown in Figure 2b is observed. Superimposed on the data is a fitting of the spectrum to three Gaussian-shaped inhomogeneously broadened bands, using the fitting procedure described in the Materials and Methods section (*15*) that compensates for band distortion by rapid-passage effects. The band center frequencies and half-widths are listed in Table 1.

Assignment of the ZFS *D* and *E* parameters of 5HW is based on the sublevel kinetic parameters that are obtained from MIDP measurements which also were carried out and analyzed globally by a procedure described recently (*12*). Global analysis yields both sublevel decay constants (k_i) and slr rate constants (W_{ij}) independently; these data are not presented in this paper, but were used in assigning the ZFS parameters of each sample. *D* and *E* (Table 1) are assigned in such a way that the T_z sublevel (the *z*-axis is normal to the plane of the chromophore) is the lowest in energy and has the smallest decay constant; both criteria are characteristic of $^3(\pi, \pi^*)$ states. *D* is positive for $^3(\pi, \pi^*)$ states and *E* is assigned to be positive for tryptophan (*17*); with this convention for *E*, the in-plane principal *x*-axis of tryptophan is approximately normal to the ethylenic double bond (*18*, *19*). For consistency, we also take E to be positive in each of the tryptophan analogues without, however, specifying the orientation of the *x*-axis.

When the phosphorescence of 5HW-V66W is monitored at 411 nm (to the blue of the shoulder at 413 nm in order to avoid emission from a red-shifted site, see below), the steady-state ODMR spectrum shown in Figure 2d is observed. Analysis of this spectrum as described above yields the parameters presented in Table 1. These parameters are assigned to 5HW at position 140 since they are similar to those of 5HW-nuclease. When the emission is monitored at 417 nm, however, the ODMR spectrum shown in Figure 2e is observed. The broad, negative polarity band at about 3.5 GHz is assigned to the $D + E$ transition of the blue-shifted 5HW at position 140. The three remaining relatively narrow bands are assigned to the red-shifted 5HW at position 66. It is interesting that although this spectrum reveals clearly the $D + E$ transition of 5HW 140, there is no evidence for its 2*E* band which should be found at about 1.3 GHz. When the monitored wavelength of 5HW-nuclease is shifted from the 0,0-band peak at 413 nm to about 419 nm, the 2E band of 5HW 140 vanishes (possibly due to extreme broadening), although the two higher-frequency bands are still observable (spectrum not shown). There is probably a significant contribution of the $D - E$ transition of 5HW 140 to the 2.5 GHz band that is assigned to the 2*E* transition of 5HW at position 66, so the analysis represented by the superimposed smooth curve, Figure 2e, should be viewed with some caution. The results of the analysis of the steady-state ODMR are given in Table 1. Assignments of *D* and *E* for 5HW 66 in 5HW-V66W were made as outlined above for 5HW-nuclease.

The slow-passage ODMR spectrum of 5HW-V66W′ (not shown) is poorly resolved; it is similar to spectra from the solvent-exposed free amino acid, independent of monitored wavelength, bearing no resemblance to the ODMR spectrum assigned to 5HW at position 66 in 5HW-V66W. The spectrum suggests that 5HW-V66W′ retains little if any structural integrity.

Table 1: Zero Field Splitting Parameters of 5HW in Staphylococcal Nuclease

		$D - E$[a]		$2E$[a]		$D + E$[a]			
sample and monitored wavelength (nm)	λ_{0-0} (nm)	ν_0 (GHz)	$\nu_{1/2}$ (MHz)	ν_0 (GHz)	$\nu_{1/2}$ (MHz)	ν_0 (GHz)	$\nu_{1/2}$ (MHz)	D (GHz)	E (GHz)
5HW-nuclease (413)	413	2.391(4)	153(3)	1.209(7)	237(6)	3.44(1)	164(15)	2.916	0.564
5HW-V66W[b] (411)	413	2.376(4)	104(5)	1.335(6)	253(7)	3.45(1)	87(9)	2.913	0.602
5HW-V66W[c] (417)	417	1.785(1)	33.3(8)	2.484(2)	126(2)	4.265(4)	40(6)	3.025	1.241
5HW[d] (412)	412	2.30	186	1.43	415	3.55	194	2.92	0.67
W[e] (406.6)	406.6	1.763(3)	58(1)	2.514(10)	146(6)	4.250(7)	81(4)	3.007	1.250

[a] Standard deviations in last digit (σ_d) given in parentheses. All parameters obtained from steady-state ODMR (*15*) unless otherwise stated. [b] Blue-shifted site, ODMR monitored to the blue of the emission maximum at 413 nm to minimize effect of the red-shifted site. [c] Red-shifted site, monitored at 0,0−band peak. [d] Free 5-hydroxytryptophan. [e] Free tryptophan. Values are from delay ODMR measurements (*11*).

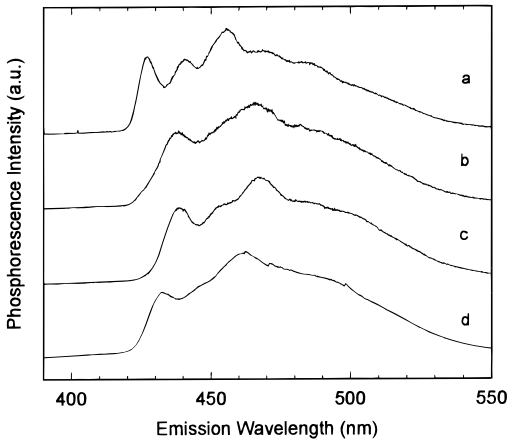

FIGURE 3: Phosphorescence spectra of (a) 7AW-nuclease, (b) 7AW-V66W, (c) 7AW-V66W′, and (d) free 7AW amino acid at 77 K using red-edge excitation; see text for a−c. Excitation wavelength of d was 295 nm using 16 nm band-pass.

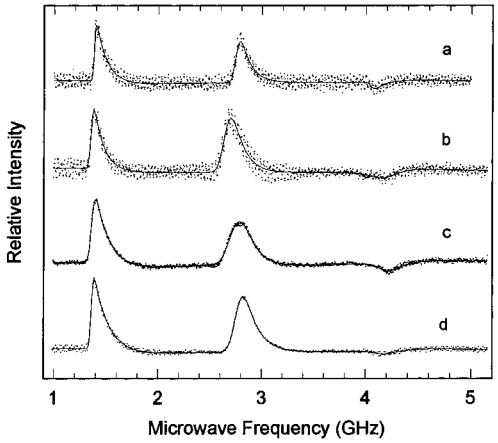

FIGURE 4: Steady-state ODMR spectra of (a) 7AW-nuclease, (b) 7AW-V66W′, (c) 7AW-V66W, and (d) free 7AW amino acid at 1.2 K. The phosphorescence is monitored at (a) 426.4, (b) 439.4, (c) 438.8, and (d) 432.5 nm using 3 nm band-pass. The microwave frequency was swept at (a) 80, (b) 80, (c) 100, and (d) 100 MHz/s, and signal averaging (40−60 accumulations) was carried out. The superimposed solid lines are the calculated best fit of each experimental spectrum to eq 1 (*15*). The values of ν_0 and $\nu_{1/2}$, obtained from delay ODMR (*11*, spectra not shown), are listed in Table 2.

Phosphorescence of 7-Azatryptophan in Staphylococcal Nuclease. The phosphorescence of 7AW in 7AW-nuclease obtained by red-edge excitation is shown in Figure 3a. The well-resolved 0,0-band of 7AW at position 140 occurs at 426.4 nm. This is a blue shift of 6.1 nm relative to its value for the free amino acid in EG/buffer glass (Figure 3d). The red-edge-excited phosphorescence of 7AW-V66W and 7AW-V66W′ is shown in Figure 3, parts b and c, respectively. The 0,0-band is red-shifted and the vibronic structure is more poorly resolved relative to 7AW-nuclease; the spectra resemble qualitatively that of the free amino acid in EG/buffer (Figure 3d) although their 0,0-bands are shifted even farther to the red. Attempts to resolve the emissions of 7AW at positions 66 and 140 as described above for 5HW did not succeed; clearly the spectrum of 7AW 140 undergoes a significant change upon introducing the analogue at position 66. As with the 5HW analogues, excitation at 295 nm induced the appearance of a 0,0-band near 407 nm and of ODMR spectra characteristic of tryptophan (spectra not shown) confirming the presence of unmodified enzyme as a component in these samples.

Optical Detection of Magnetic Resonance of 7-Azatryptophan in Staphylococcal Nuclease. Slow-passage ODMR spectra of 7AW were measured for each of the samples, monitoring the peak of the phosphorescence 0,0-band. The steady-state spectra are presented in Figure 4 and were analyzed to compensate for rapid-passage effects (*15*). The analyses are represented by the smooth curves superimposed on the data in Figure 4. The major portion of the "noise" observed in these spectra is actually coherent modulation produced by the rotating sector which could not be eliminated entirely by signal averaging. Because of the large fluorescence component of 7AW luminescence, in contrast with 5HW, phosphorescence had to be isolated by a rotating sector. The band center frequencies and half-widths of these samples obtained from analyses of delay ODMR spectra (*11*) (not shown) are listed in Table 2. In contrast with the results obtained above for the 5HW-modified enzyme, no clear resolution of distinct sites could be found for 7AW-V66W, Figure 4c, suggesting the loss of much of the structural integrity of this mutant enzyme as a result of the 7AW modification. A slight broadening of the $2E$ transition suggests some site heterogeneity, however. We examined the $D - E$ signal of 7AW-V66W′ (Figure 4b) carefully using the delay ODMR method (*11*). Under increasingly slow passage conditions, the delay ODMR $D - E$ signal of 7AW-V66W′ reveals structure that we have analyzed into two Gaussian bands, with center frequencies of 1.337 and 1.373 GHz, as shown in Figure 5. The widths of the component bands (Figure 5 caption) are comparable to those found for 7AW-nuclease and for the free amino acid (Table 2) and suggest the presence of two major conformational forms of 7AW-V66W′.

Phosphorescence of 4-, 5-, and 6-Fluorotryptophans in Staphylococcal Nuclease. The phosphorescence spectra of the 4FW-, 5FW-, and 6FW-containing samples measured at 1.2 K are shown in Figures 6, 7, and 8, respectively. Each

Table 2: Zero Field Splitting Parameters of 7AW in Staphylococcal Nuclease

		$D - E^a$		$2E^a$		$D + E^a$			
sample	λ_{0-0} (nm)	ν_0 (GHz)	$\nu_{1/2}$ (MHz)	ν_0 (GHz)	$\nu_{1/2}$ (MHz)	ν_0 (GHz)	$\nu_{1/2}$ (MHz)	D (GHz)	E (GHz)
7AW-nuclease	426.4	1.389(1)	14(1)	2.801(20)	40(7)	4.168(20)	36(4)	2.780	1.395
7AW-V66W′	439.6	1.373 (3)[b]	12.4 (10)[b]	2.636(3)	70(10)	4.103(2)	142(6)	2.723[c]	1.349[c]
		1.337 (3)[b]	11.8 (7)[b]						
7AW-V66W	438.8	1.336(2)	21(2)	2.680(9)	89(7)	4.127(10)	120(10)	2.732	1.368
7AW[d]	432.5	1.354(1)	15.9(3)	2.735(3)	55(6)	4.097(10)	82(4)	2.726	1.370

[a] Standard deviation in last digit (σ_d) given in parentheses. All parameters obtained from delay ODMR by monitoring $\lambda_{0,0}$ (*11*). [b] Resolved doublet. [c] Values based on weighted average of $D - E$ frequencies. [d] Free amino acid. Values taken from ref *11*.

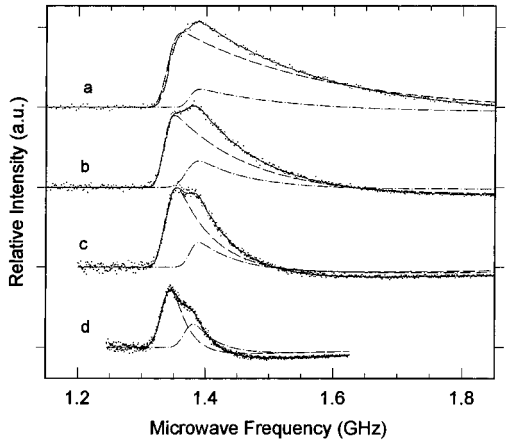

FIGURE 5: Delay ODMR responses of 7AW-V66W′ at 1.2 K. The microwave frequency is swept through the $D - E$ transition at a rate of (a) 130, (b) 70, (c) 40, and (d) 20 MHz/s, and the frequency is limited by a 2.0 GHz low-pass filter. The superimposed solid lines are best fits to the delayed ODMR theoretical expression (*11*) assuming two components whose individual responses are fitted with (- - -) and (-·-·-·). The average best-fit {ν_0 (GHz), $\nu_{1/2}$ (MHz)}, with standard deviations of last digit given in parentheses, are {1.337(3), 12.4(10)} and {1.373(3), 11.8(7)}.

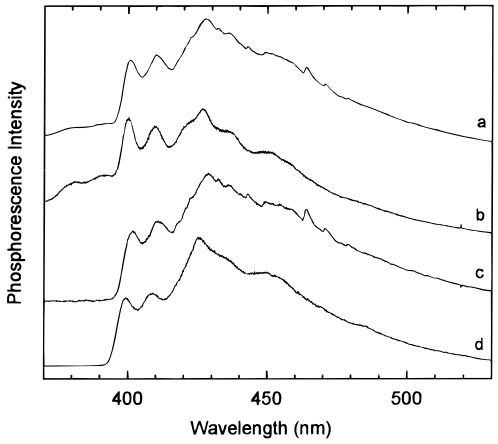

FIGURE 6: Phosphorescence spectra at 1.2 K of (a) 4FW-V66W, (b) 4FW-nuclease, (c) 4FW-V66W minus 4FW-nuclease, and (d) free 4FW amino acid. An excitation wavelength of 285 nm was used.

free amino acid (Figures 6d, 7e, and 8e) reveals a clearly resolved 0,0-band that peaks at 399, 408.2, and 411 nm, respectively. Each FW-nuclease spectrum, 6b, 7b, and 8b, exhibits increased resolution relative to the free amino acid, with only a small (1−2 nm) red shift. Because of the blue-shifted absorption edge of 4FW that required excitation at about 285 nm, a poorly resolved blue-shifted phosphorescence component that originates from tyrosine is apparent in Figure 6, parts a and b, but is absent in Figures 7 and 8

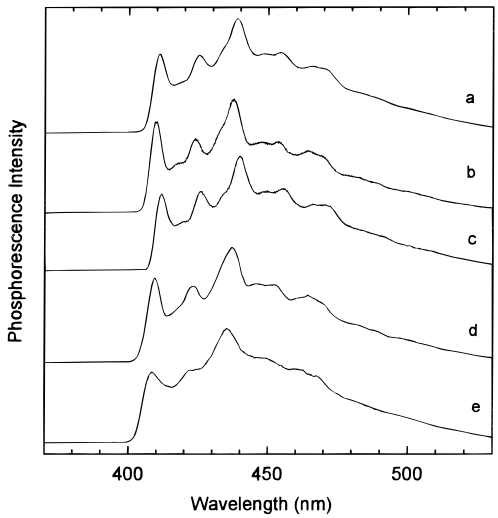

FIGURE 7: Phosphorescence spectra at 1.2 K of (a) 5FW-V66W, (b) 5FW-nuclease, (c) 5FW-V66W minus 5FW-nuclease (d) 5FW-V66W′, and (e) free 5FW amino acid. An excitation wavelength of 302 nm, 16 nm band-pass, and a WG305-1 cutoff filter were used.

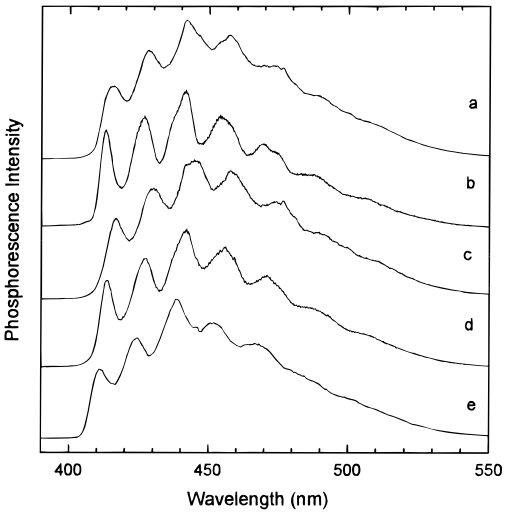

FIGURE 8: Phosphorescence spectra at 1.2 K of (a) 6FW-V66W, (b) 6FW-nuclease, (c) 6FW-V66W minus 6FW-nuclease (d) 6FW-V66W′, and (e) free 6FW amino acid. Excitation conditions are the same as those given in the Figure 7 caption.

for which the excitation was shifted to the red. The spectra of the FW-V66W mutants, Figures 6a, 7a, and 8a, each exhibit broadening and a red shift of the FW 0,0-band relative to the corresponding FW-nuclease that reflect the introduction of FW at position 66. A representation of the phosphorescence spectrum of FW 66 in each FW-V66W mutant was obtained by subtracting from its spectrum a scaled FW-nuclease spectrum. As for 5HW, the scaling was based on

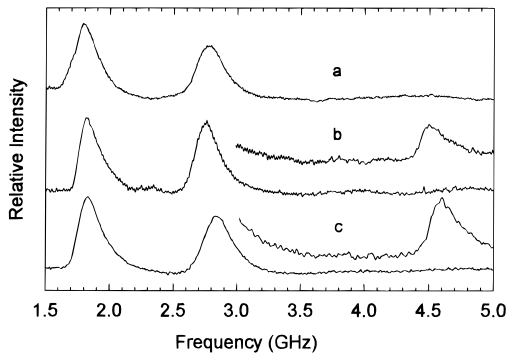

FIGURE 9: Steady-state ODMR spectra of (a) 4FW-V66W monitored at 400 nm, (b) 4FW-nuclease at 400 nm, and (c) free 4FW amino acid at 399 nm. The inserts in b and c show the $D + E$ transition that is induced by saturating the low-frequency $D - E$ transition with a second microwave sweeper (EEDOR). Excitation was at 285 nm.

the assumptions that the FW 140 spectrum is unchanged by introduction of a second FW at position 66 and that it has the same quantum yield as FW 66. These difference spectra are plotted as Figures 6c, 7c, and 8c. The 0,0-band of the difference spectrum is found to be shifted to the red of the FW-nuclease spectrum in each case, as expected on the basis of the red shift of each FW-V66W spectrum relative to FW-nuclease. The difference spectrum is probably the most reliable in the case of 6FW which produces the largest red shift at position 66 relative to position 140. The spectra of the 5FW−V66W′ and 6FW-V66W′ fragments are shown in Figures 7d and 8d, respectively. The 0,0-bands of these spectra are each shifted to the blue relative to the corresponding FW-V66W difference spectrum, implying that the local environments of 5FW 66 and 6FW 66 are altered significantly upon formation of the V66W′ fragment.

The presence of residual tryptophan-containing protein would be very difficult or impossible to detect from the phosphorescence since the 4FW, 5FW, and 6FW spectra occur in the same wavelength region as that of tryptophan. Moderate red-edge excitation (see Materials and Methods) of the 5FW- and 6FW-containing proteins discriminates against the excitation of tryptophan emission, but we cannot rule out a tryptophan component in the phosphorescence of the 4FW-containing samples. The 0,0-band of residual tryptophan would overlap with the first resolved vibronic band of 4FW-nuclease and 4FW-V66W (Figure 6, parts b and a, respectively). On the other hand, evidence for the presence of a tryptophan component in the emission of 4FW-V66W is found using ODMR (see below).

Optically Detected Magnetic Resonance of Fluorotryptophan in Staphylococcal Nuclease. (A) 4-Fluorotryptophan. The steady-state ODMR spectra of the 4FW, 4FW-nuclease, and 4FW-V66W samples are shown in Figure 9. The broad phosphorescence background observed for 4FW-nuclease and 4FW-V66W (Figure 6a,b), attributed to tyrosine, did not adversely affect the ODMR spectra in the 4FW frequency region. Under normal conditions of the steady-state ODMR experiment, the $D + E$ transitions were not visible. However, they could be observed clearly by EEDOR, saturating the $D - E$ band with a second microwave sweeper. The ODMR spectra of 4FW-nuclease and 4FW-V66W resemble that of the free amino acid; distinct sites are suggested in the latter (Figure 9a) by the increased bandwidth of the $D - E$ and $2E$ transitions. These bands were deconvoluted as doublets (*15*) fixing the parameters of one site at those found from analysis of 4FW-nuclease yielding parameters for position 66 that differ slightly from those of position 140 in 4FW-nuclease (Table 3). The ZFS parameters D and E of 4FW-nuclease are reduced below those of the free amino acid, and the line widths are narrower (Table 3), suggesting that 4FW occupies a structured site in 4FW-nuclease. When the phosphorescence of 4FW-V66W (Figure 6a) is monitored at the peak of the first resolved vibronic band, 409 nm, the $D - E$ and $2E$ bands develop a structure consistent with the superpositon of the 4FW-V66W spectrum (Figure 9a) and the W-V66W spectrum (Figure 2c). Although we did not attempt to deconvolute these ODMR bands (not shown) by computer, their appearance strongly supports the presence of residual W-V66W in the sample.

(*B*) *5-Fluorotryptophan.* The ODMR spectra of 5FW and the 5FW-containing nuclease samples are presented in Figure 10. 5FW-V66W (Figure 10a) clearly shows resolution of distinct 5FW sites, whereas 5FW-nuclease reveals only a single site (Figure 10b) whose ODMR consists of a poorly resolved pair of signals ($D - E$ and $2E$). An additional $D + E$ signal, shown as an insert, is induced by EEDOR. The ODMR spectrum associated with 5FW at position 66 of 5FW-V66W, obtained by subtracting a scaled down spectrum 10b from 10a by computer, is shown as spectrum 10a*. This spectrum reveals well-resolved $D - E$ and $2E$ bands, assigned to 5FW in position 66, in contrast with the poorly resolved pair of the 5FW-nuclease. The ZFS of 5FW at position 140 in 5FW-nuclease and in 5FW-V66W resemble those of the free amino acid (Figure 10d, Table 3), whereas the ZFS of 5FW at position 66 differ considerably (Table 3). Figure 10c, the ODMR spectrum of 5FW-V66W′, reveals a poorly resolved doublet in the $D - E$, $2E$ band region and thus resembles the spectrum of 5FW-nuclease and the free amino acid more closely than that of 5FW 66 of 5FW-V66W (Figure 10a*). The ZFS differ significantly, however, from those of the latter two 5FWs (Table 3). Because of the overlap of the $D - E$ and $2E$ bands of these samples, delay ODMR was used to obtain accurate ν_0 and $\nu_{1/2}$ values for the $D - E$ transition. With delays of 20 s or longer, both T_x and T_y sublevel populations have decayed to undetectable levels, leaving only T_z populated. Thus, only the $D - E$ signal is observed in the $D - E$, 2E region since the $2E$ ($T_x \leftrightarrow T_y$) band has vanished. The $D - E$, $2E$ signal region of 5FW-V66W under these (long) delay ODMR conditions is shown in Figure 11. It reveals clearly the $D - E$ bands of the two 5FW sites, and is analyzed as a composite of two transitions from independent triplet states, as outlined earlier in the Methods section. Figure 11 should be compared with the corresponding frequency region of Figure 10a.

(*C*) *6-Fluorotryptophan.* The ODMR spectra of the 6FW-containing samples are given in Figure 12. Of all the tryptophan analogues studied in this work, the poorest ODMR signal quality was found for 6FW. The spectrum of the free amino acid, 6FW, is shown in Figure 12d. The $D - E$ and $2E$ bands are well-resolved, and EEDOR produces the $D + E$ band. The same bands are observed in 6FW-nuclease (Figure 12b), but frequency shifts are observed and the bands are narrower, indicating less inhomogeneous broadening (Table 3). The large wavelength shift between

Table 3: Zero Field Splitting Parameters of Fluoro-W in Staphylococcal Nuclease

		$D - E$[a]		$2E$[a]		$D + E$[a]			
sample and monitored wavelength (nm)	λ_{0-0} (nm)	ν_0 (GHz)	$\nu_{1/2}$ (MHz)	ν_0 (GHz)	$\nu_{1/2}$ (MHz)	ν_0 (GHz)	$\nu_{1/2}$ (MHz)	D (GHz)	E (GHz)
4FW (399)	399	1.765(2)	56(3)	2.75(1)	98(3)	4.51(1)	65.7(3)	3.14	1.37
4FW-nuclease (400)	400	1.767(1)	42.3(6)	2.672(7)	75(1)	4.430(8)	53(6)	3.10	1.33
4FW-V66W (400) position 140	400	*b*	*b*	*b*	*b*	*b*	*b*	3.10	1.33
4FW-V66W (400) position 66	402[c]	1.727(3)[d]	54(4)[d]	2.71(1)[d]	70(1)[d]	4.44[e]		3.09	1.36
5FW (408.5)	408.5	1.924(2)	73(3)	2.250(6)	133(8)	4.163(2)	83(8)	3.04	1.12
5FW-nuclease (409)	409	1.926(2)[f]	55(2)[f]	2.122(1)	103(7)	4.05(1)	63(2)	2.99	1.06
5FW-V66W (412) position 140	409	1.907(1)[f]	*b*	*b*		4.03[e]		2.97	1.06
5FW-V66W (412) position 66	412[c]	1.777(1)[f]	36.3(1)[f]	2.381(3)[g]	35.3(1)[g]	4.16[e]		2.97	1.19
5FW-V66W′ (409.5)	409.5	1.912(2)[f]	49(1)[f]	2.15[e]		4.064(6)	51(8)	2.99	1.08
6FW (411)	411	1.654(1)	43.6(9)	2.635(3)	87(2)	4.289(4)	57(3)	2.97	1.32
6FW-nuclease (413)	413	1.640(1)	33(2)	2.53(1)	56(5)	4.19[e]		2.90	1.26
6FW-V66W[h] (413) position 140	413	1.623(3)	75.6(4)	2.561(5)	63.8(6)	4.18[e]		2.90	1.28
6FW-V66W[h] (417) position 66	417[c]	1.528(1)	37(1)	2.687(3)	79(10)	4.22[e]		2.87	1.34
6FW-V66W′ (413.5)	413.5	1.612(2)	37(2)	2.59(3)	87(11)	4.22(1)	90(10)	2.91	1.30

[a] Standard deviations (σ_d) in last digit given in parentheses. Conventional slow-passage ODMR spectra were fitted unless otherwise stated. [b] Parameter assumed equal to that of the FW-nuclease. [c] λ_{0-0} found from a difference spectrum (see text). [d] Conventional slow-passage ODMR fitted as a sum of two species assuming parameters for position 140 equal to those in a nuclease. [e] Position not fitted, calculated from the other frequencies. [f] From delayed slow-passage analysis (*11*). [g] Obtained by fitting difference spectrum of Figure 10a* (*15*). [h] Obtained by optical selection, fitting conventional slow-passage ODMR (*15*).

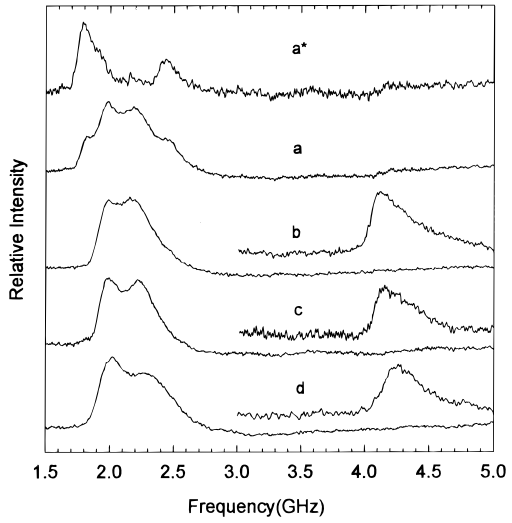

FIGURE 10: Steady-state ODMR spectra of (a) 5FW-V66W, (b) 5FW nuclease, (c) 5FW-V66W′, and (d) free 5FW amino acid. Monitored wavelengths are given in Table 3. The difference spectrum, 5FW-V66W minus 5FW-nuclease, is given as a*. The inserts in b, c, and d show the $D + E$ transition that is observed using EEDOR, saturating the $D - E$ band. Excitation conditions are given in the Figure 7 caption.

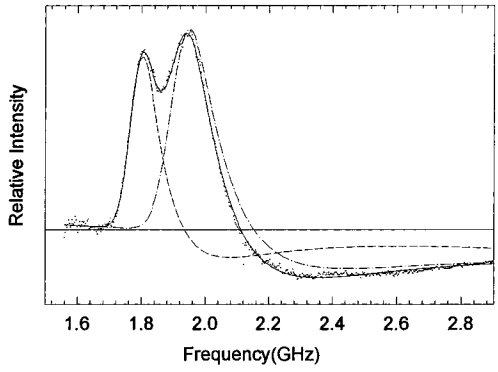

FIGURE 11: Delay ODMR responses of 5FW-V66W at 1.2 K using a 20 s delay time. The microwave frequency is swept through the $D - E$ transitions at a rate of 40 MHz/s. The superimposed solid line is the best fit to the delayed ODMR theoretical expression (*11*) assuming two components, (- - -) and (-·-·-·), for 5FW at positions 66 and 140, respectively (see Table 3).

the phosphorescence 0,0-bands of 6FW at positions 66 and 140 of 6FW-V66W (Figure 8a,b,c) allows the resolution of the ODMR spectra of these sites by optical selection. The optically selected ODMR spectrum of 6FW at position 140, obtained by monitoring the emission of 6FW-V66W at 413 nm, is given in Figure 12a, while that of 6FW at position 66 is shown in Figure 12a*, obtained by monitoring its emission at 417 nm. Assignments are based on the similarity of spectrum 12a and that of 6FW-nuclease (Figure 12b). The ZFS of 6FW 66 and 6FW 140 are clearly different in 6FW-V66W, and the bandwidths of the former are less, indicating a more homogeneous local environment (Table 3). Another significant difference between these sites is the intensity pattern of the ODMR spectra (Figure 12a vs 12a*) that are the result of differing sublevel kinetic behavior. 6FW at position 66 exhibits a prominent $D + E$ transition and its $2E$ band is very weak, while the reverse is the case for 6FW at position 140, which resembles the intensity patterns of 6FW-nuclease, 6FW-V66W′, and the free amino acid (Figure 12b,c,d, respectively).

DISCUSSION

By use of red-edge excitation, we have selectively induced the phosphorescence of 5HW- and 7AW-modified wild-type, V66W, and V66W′ Staphylococcal nuclease in the presence of a substantial amount of tryptophan-containing forms of these enzymes. Using absorbance curve fitting procedures, we have argued (*8, 9*) that the various alloproteins contain less than 10% residual tryptophan. However, the ability to see residual tryptophan phosphorescence (which we can avoid in these studies) is a result of the very sharp 0−0 transition at 405−410 nm (sharper for tryptophan than for these analogues) and of the relative efficiency of intersystem crossing to the triplet state of tryptophan versus these analogues (unknown for the latter). The fact that we can observe a sharp 0−0 transition at 405−410 nm for most of these alloproteins indicates that, despite our rosy estimates from simulated absorption spectra, these samples do contain detectable residual tryptophan; a quantitative estimate of this

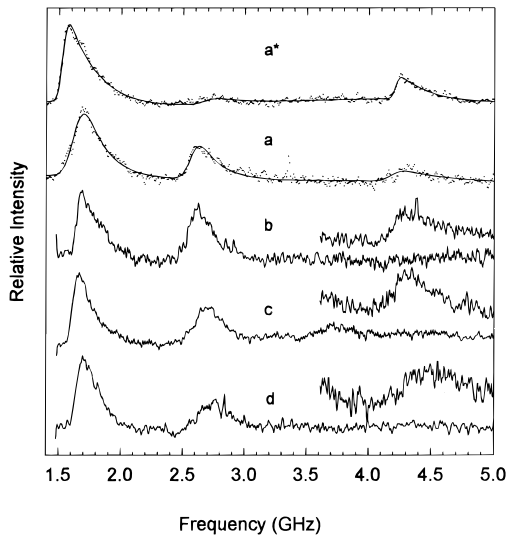

FIGURE 12: Steady-state ODMR spectra of (a) 6FW-V66W monitored at 413 nm, (a*) 6FW-V66W monitored at 417 nm, (b) 6FW-nuclease monitored at 413 nm, (c) 6FW-V66W′ monitored at 413.5 nm, and (d) free 6FW amino acid monitored at 411 nm. The inserts in b, c, and d show the $D + E$ transition that is observed by EEDOR while saturating the $D - E$ band. Excitation conditions are the same as those given in the Figure 7 caption.

tryptophan content based on the phosphorescence spectra was not attempted due to the unknown intersystem crossing efficiency of the analogues. Nevertheless, all of the ODMR and MIDP measurements of the 5HW and 7AW analogues to be discussed below were performed by exciting at the red edge, where residual tryptophan emission is avoided.

The 4FW analogues had to be excited with shorter wavelengths, and their phosphorescence spectra overlap with those of tryptophan. Evidence for the presence of residual tryptophan in 4FW-V66W was found by ODMR when monitoring the emission in the wavelength region where both 4FW and tryptophan emit. Moderate red-edge excitation of the 5FW and 6FW analogues, whose phosphorescence also overlaps with that of tryptophan, avoided producing any dectable tryptophan triplet states. In the case of the 5FW analogues, the ODMR frequencies in 5FW-nuclease and 5FW−V66W′ are sufficiently different than those of tryptophan that the latter would have been detected by ODMR, if its triplet state had been produced in significant amounts.

5-Hydroxytryptophan. Introduction of 5HW into 5HW-nuclease brings about considerable reduction in line widths relative to the free amino acid, particularly that of the 2*E* band (Table 1), although they remain quite broad relative to tryptophan either as the free amino acid or in wild-type nuclease (*13*). The major effect on the ZFS is a reduction in the *E* parameter from 0.67 to 0.56 GHz. This effect could be the result of a nonplanar distortion of the 5-hydroxyindole chromophore induced by steric forces within the protein.

The presence of two distinct 5HW sites in 5HW-V66W is apparent from a comparison of the phosphorescence spectra, Figure 1, part b versus part a. The difference spectrum, Figure 1c, with a red-shifted 0,0-band at 417 nm is a representation of the emission of 5HW at position 66. The results of this procedure suggest that the environment of 5HW 140 is relatively insensitive to the introduction of 5HW at position 66. Possible small effects of the V66W mutation on 5HW 140 are revealed, however, by optically selected ODMR measurements. When the phosphorescence is monitored at 411 nm where the emission of 5HW 66 is negligible (Figure 1c), the ODMR spectrum resembles qualitatively that of 5HW 140 in 5HW-nuclease, Figure 2, part d versus part b. The ODMR peak frequencies of the $D - E$ and $D + E$ transitions are changed only slightly from those of 5HW-nuclease, but the 2*E* frequency increases significantly (Table 1). However, as pointed out above, the 2*E* band frequency is particularly sensitive to the monitored wavelength; possibly some or all of the shift in this case can be attributed to the difference in monitored wavelength (411 vs 413 nm) rather than a modification of the local environment.

Monitoring the phosphorescence of 5HW-V66W at 417 nm produces the spectrum shown in Figure 2e, which reveals not only the broad, negative polarity $D + E$ band of 5HW 140 at 3.5 GHz but also three narrower bands that we have assigned to 5HW 66. The band peak frequencies, listed in Table 1, are strikingly different from those of 5HW 140, or of the free amino acid. The largest change is in the ZFS *E* parameter which doubles in magnitude. The ZFS do not resemble those of 5HW as much as they do those of tryptophan, which can be ruled out as the origin of these bands, however, for the following reasons. (1) Red-edge excitation was used, which does not produce detectable amounts of tryptophan luminescence. (2) When excitation was shifted to 295 nm, a new phosphorescence band appeared at 407 nm which, when monitored, produced the tryptophan ODMR spectrum shown in Figure 2c. This spectrum clearly differs from that of Figure 2e, since the $D - E$ and 2*E* bands are doublets, and no $D + E$ band is apparent. A spectrum identical to Figure 2c has been reported previously (*13*) from a sample of authentic W-V66W.

The resemblance of the properties of 5HW 66 in 5HW-V66W to those of tryptophan, rather than to 5HW 140, or to the free amino acid suggests that a significant change in the electronic character of the triplet state is induced by local interactions with the protein. The large value of *E* that characterizes the triplet state of tryptophan is attributed to major delocalization of π-electron spin density into the ethylenic double bond of the five-membered ring (*20*, *21*). 5-Hydroxyl substitution leads to a large reduction of spin density in the ethylenic bond that must be associated with a change in the electronic character of the lowest-energy triplet state. The effect of the 5-hydroxyl on the electronic distribution is reversed by a specific interaction at position 66 of 5HW-V66W, the resulting distribution being similar to that of tryptophan. The nature of this interaction is not understood at present. The effects of various substituents on the triplet-state properties of tryptophan are being investigated.

7-Azatryptophan. Incorporation of 7AW into 7AW-nuclease leads to considerable narrowing of the ODMR bands (Table 2), suggesting an increase in the homogeneity of the microenvironment relative to the aqueous solvent. Both the *D* and *E* parameters increase by 2%, consistent with an overall contraction of the electronic distribution, $\langle(r^2 - 3z^2)/r^5\rangle_{av}$ and $\langle(y^2 - x^2)/r^5\rangle_{av}$, each increasing by about 2%. The phosphorescence spectrum also becomes narrower, and the 0,0-band is shifted to the blue by 6 nm (Figure 3, Table 2). This is in contrast with W-nuclease (*13*) where the tryptophan 0,0-band undergoes a slight (ca. 0.6 nm) *red* shift relative

to the free amino acid. The ODMR properties of 7AW-nuclease indicate that the enzyme has structural integrity, at least in the vicinity of 7AW 140.

In 7AW-V66W, on the other hand, the line widths increase relative to the free amino acid in aqueous solvent (Table 2) indicating even greater heterogeneity. In contrast with W-V66W and 5HW-V66W, however, we cannot distinguish between 7AW at positions 66 and 140 by ODMR. We conclude that the heterogeneity at each site is sufficient to mask small differences that may be present. The red shift of the phosphorescence of 7AW-V66W with respect to 7AW-nuclease even beyond that of the free amino acid (Figure 3, Table 2) and the shift of the ZFS to those of the free amino acid (Table 2) indicate that the structural integrity of the protein near 7AW 140 has been compromised. The triplet-state properties of 7AW-V66W do not provide evidence that the protein has a unique structure, although the 7AW triplet-state properties are distinguishable from those of the free amino acid.

In the fragment 7AW-V66W′, only 7AW 66 is present. The triplet-state properties differ noticeably from those of 7AW-V66W and the free amino acid. Specifically, *E* is reduced significantly relative to these samples (Table 2). Distinct sites are resolved by delay ODMR at reduced sweep rates as shown in Figure 5. The widths of the individual bands are quite narrow, even narrower than is found for this transition in 7AW-nuclease, which appears to have a discrete structure. The narrow bandwidths indicate that each site has a more homogeneous environment than is found in 7AW-nuclease or in solvent-exposed 7AW. It appears from this result that 7AW-V66W′ folds into two major structural types that can be resolved by ODMR. This resolution is assisted by the extremely narrow width of the $D - E$ ODMR band of 7AW. The other ODMR bands of 7AW-V66W′ could not be resolved in this manner, possibly because of their greater susceptibility to inhomogeneous broadening.

4-, 5-, and 6-Fluorotryptophan. Considerable narrowing of the ODMR bands of the FW-nucleases is observed relative to the free amino acids as was the case for 7AW-nuclease. The *D* and *E* parameters both decrease slightly (in contrast with 7AW, where increases are found). The resolution of the phosphorescence spectra increases, but the 0,0-band is shifted only slightly to the red. The wild-type nuclease structural integrity does not appear to be affected by FW substitution at position 140.

The triplet-state properties of 4FW appear to be the least sensitive of all the analogues investigated to changes in the local environment. Phosphorescence shifts (only about 2 nm between sites 140 and 66) as well as site-influenced ZFS shifts are small, rendering this analogue not very useful as a triplet-state probe.

For the 5FW- and 6FW-V66W mutants, in contrast with 7AW-V66W, the ODMR linewidths decrease relative to the free amino acids, indicating increased homogeneity. In each case we could distinguish the FW residues at positions 66 and 140 both in phosphorescence and in ODMR. These results indicate that structural integrity of the V66W nuclease is retained with 5FW or 6FW at both position 66 and position 140. The phosphorescence of 5FW or 6FW at the 66 position is shifted to the red relative to that of position 140. The largest shift (4 nm) is observed for 6FW. Concerning the ZFS parameters of 5FW and 6FW, *D* undergoes a small decrease, but *E* increases substantially as the residue is moved from position 140 to position 66. Both *D* and *E* are considerably smaller in position 140 than they are for the free amino acid in solution. The latter appears to be the case also for 4FW, but the spectral shifts between nuclease sites are much smaller than for 5FW and 6FW.

The fragments 5FW- and 6FW-V66W′ produce more highly resolved phosphorescence than do the free amino acids. For the 5FW analogue, in particular, the ODMR line widths are narrower than those of the free amino acid. However, the ODMR parameters and phosphorescence spectra differ from those observed for position 66 in the intact V66W mutants. Thus, although each fragment shows considerable homogeneity of the local environment, and thus indicates a structured environment near position 66, this structure is differentiated readily from that of the intact mutant.

CONCLUSIONS

The results obtained in this paper demonstrate the power of phosphorescence and ODMR spectroscopy to characterize tryptophan-like molecules and to distinguish their properties when incorporated at distinct sites in proteins. The results of these measurements have been used to draw inferences about the effects of substituting tryptophan analogues on the structural integrity of Staphylococcal nuclease, the V66W mutant, and V66W′, its Δ137−149 fragment.

By focusing on the tryptophan positions, these phosphorescence and ODMR data complement the thermodynamic information in the preceding article (*10*). For example, denaturant and thermal unfolding studies show that 7AW has a destabilizing effect when incorporated into either position 140 or position 66 of these proteins. However, the thermodynamic studies do not reveal whether a particular tryptophan analogue (e.g., 7AW) experiences a structured environment, regardless of the degree of perturbation of the global stability of the protein. The triplet-state measurements provide fingerprint type data, due to the sharp 0−0 phosphorescence transition, its environmental sensitivity, and that of the ZFS parameters which can characterize the structural homogeneity/heterogeneity as well as polarity and polarizability of the tryptophan sites.

For the nuclease systems studied here, the following inferences can be made about their structural integrity. Incorporation of any one of the analogues, 5HW, 7AW, 4FW, 5FW, or 6FW, at the W140 position of wild-type nuclease leads to a protein that retains structure at this site. As far as the mutant nuclease V66W is concerned, phosphorescence and ODMR provide evidence that structure is retained at sites 66 and 140 when the 5HW, the 5FW, and the 6FW analogues are incorporated. The structure of site 140 is not noticeably altered by the V66W mutation except in the presence of the analogue 7AW. Structural integrity of both sites is lost upon incorporation of 7AW. In the case of the V66W′ fragment, we have found that site 66 is structured in the presence of 7AW, 5FW, and 6FW, but this structure can be differentiated in each case from the structure of site 66 in the intact mutant nuclease, V66W. In the case of 7AW, two distinct site 66 structures can be resolved using ODMR spectroscopy. In previous work on the tryptophan-containing proteins (*13*) we found that site 66 of the V66W′

fragment is structured but also can be differentiated from site 66 in intact V66W. 5HW-V66W′, on the other hand, appears to be unstructured from our present results.

A unique perturbation of the triplet-state ZFS of 5HW takes place when it is incorporated at position 66 of 5HW-V66W. The relatively small *E* parameter characteristic of the free amino acid and of 5HW at position 140 doubles in magnitude. It is interesting to recall that incorporation of 5HW into V66W causes significant global stabilization of this mutant protein (*10*). This change in ZFS is mirrored, although to a smaller extent, by the other 5-substituted derivative, 5-FW, whose *E* value increases substantially when placed in site 66 of V66W. This specific interaction with the protein at this site is eliminated upon formation of the V66W′ fragment. The nature of the interaction between 5HW or 5FW and the protein at position 66 that produces these large ZFS changes is not now understood but is under investigation.

In addition to the results presented in this paper, we have characterized fully the triplet-state decay kinetics of each system studied using global analysis of MIDP responses (*12*). These results will be published separately.

REFERENCES

1. Hogue, C. W. V., Rasquinha, I., Szabo, A. B., and MacManus, J. P. (1992) *FEBS Lett. 310*, 269−272.
2. Ross, J. B. A., Senear, D. F., Waxman., E., Kombo, B. B., Rusinova, E., Huang, Y. T., Laws, W. R., and Hasselbacher, C. A. (1992) *Proc. Natl. Acad. Sci. U.S.A. 89*, 12023−12027.
3. Soumillion, P., Jespers, L., Vervoot, J., and Fastrez, J. (1995) *Protein Eng. 8*, 451−456.
4. Ross, J. B. A., Szabo, A., and Hogue, C. W. V. (1997) *Methods Enzymol. 278*, 151−190.
5. Pratt, F. A., and Ho, C. (1975) *Biochemistry 14*, 3035−3040.
6. Hoetlzi, S. D., and Frieden, C. (1996) *Biochemistry 35*, 16843−16851.
7. Danielson, M. A., and Falke, J. J. (1996) *Annu. Rev. Biophys. Biomol. Struct. 25*, 163−195.
8. Wong, C.-Y., and Eftink, M. R. (1997) *Protein Sci. 6*, 689−697.
9. Wong, C.-Y., and Eftink, M. R. (1998) *Biochemistry 37*, 8938−8946.
10. Wong, C.-Y., and Eftink, M. R. (1998) *Biochemistry 37*, 8947−8953.
11. Wu, J. Q., Ozarowski, A., Davis, S. K., and Maki, A. H. (1996) *J. Phys. Chem. 100*, 11496−11503.
12. Ozarowski, A., Wu, J. Q., and Maki, A. H. (1996) *J. Magn. Reson., Ser. A 121*, 178−186.
13. Eftink, M. R., Ionescu, R., Ramsay, G. D., Wong, C.-Y., Wu, J. Q., and Maki, A. H. (1996) *Biochemistry 35*, 8084−8094.
14. Kwiram, A. L. (1982) in *Triplet State ODMR Spectroscopy*, (Clarke, R. H., Ed.) pp 427−478, Wiley, New York.
15. Wu, J. Q., Ozarowski, A., and Maki, A. H. (1996) *J. Magn. Reson., Ser. A 119*, 82−89.
16. Kuan, T. S., Tinti, D. S., and El-Sayed, M. A. (1970) *Chem. Phys. Lett. 4*, 507−510.
17. Maki, A. H. (1995) *Methods Enzymol. 246*, 610−638.
18. Zuclich, J. (1970) *J. Chem. Phys. 52*, 3592−3596.
19. Smith, C. A., and Maki, A. H. (1993) *J. Phys. Chem. 97*, 997−1003.
20. Kochanski, E., and Pullman, A. (1969) *Int. J. Quantum Mech. 3*, 1055.
21. Harrigan, E. T., and Hirota, N. (1975) *J. Am. Chem. Soc. 97*, 6647−6652.

BI9718649